Meshless Local Petrov-Galerkin Method for Heat Conduction Problem in an Anisotropic Medium

J. Sladek[1], **V. Sladek**[1], **S.N. Atluri**[2]

Abstract: Meshless methods based on the local Petrov-Galerkin approach are proposed for solution of steady and transient heat conduction problem in a continuously nonhomogeneous anisotropic medium. Fundamental solution of the governing partial differential equations and the Heaviside step function are used as the test functions in the local weak form. It is leading to derive local boundary integral equations which are given in the Laplace transform domain. The analyzed domain is covered by small subdomains with a simple geometry. To eliminate the number of unknowns on artificial boundaries of subdomains the modified fundamental solution and/or the parametrix with a convenient cut-off function are applied. In the formulation with Heaviside step function the final form of local integral equations has a pure contour character even for continuously nonhomogeneous material properties. The moving least square (MLS) method is used for approximation of physical quantities in LBIEs.

keyword: meshless method, local weak form, Heaviside step function, fundamental solution, moving least squares interpolation, Laplace transform

1 Introduction

Introducing new advanced materials into many fields of engineering it is increasingly growing the necessity to solve boundary value problems in anisotropic and continuously nonhomogeneous solids. Conventional computational methods with domain (FEM) or boundary (BEM) discretizations have their own drawbacks to solve such kind of problems. Conventional boundary element method (BEM) is efficient to use mainly to problems where the fundamental solution is available. Since new composite materials are frequently used for structures

under a thermal load, it is indispensable to analyze their thermal properties. The heat conduction problem in a homogeneous body with isotropic material properties was successfully solved by the BEM very frequently in literature [Brebbia et al. (1984)]. A pure boundary formulation is available even for anisotropic media [Chang et al. (1973)]. However, the fundamental solution for continuously nonhomogeneous bodies is not available in generally. If an exponential spatial variation of material properties is considered, one can derive the fundamental solution for heat conduction problems [Sutradhar et al. (2002)].

In spite of the great success of the finite and boundary element methods as effective numerical tools for the solution of boundary value problems on complex domains, there is still a growing interest in development of new advanced methods. Many meshless formulations are becoming to be popular due to their high adaptivity and a low cost to prepare input data for numerical analysis. Number of methods has been proposed so far. The first attempt to document the state of the art of this growing family of numerical procedures was given by [Belytschko et al. (1994)] and in recent monographs by [Atluri and Shen (2002b), Atluri (2004)]. A variety of meshless methods has been proposed so far. Many of them are derived from a weak-form formulation on global domain [Belytschko et al. (1994)] or a set of local subdomains [Atluri and Shen (2002a,b), Sladek et al. (2001), (2002), (2003)]. In the global formulation background cells are required for the integration of the weak form. In methods based on local weak-form formulation no cells are required and therefore they are often referred to call as truly meshless methods. If for the geometry of subdomains a simple form is chosen, numerical integrations can be easily carried out over them. The meshless local Petrov-Galerkin (MLPG) method [Atluri (2004)] is fundamental base for the derivation of many meshless formulations, since trial and test functions are chosen from different functional spaces. If the test func-

[1] Institute of Construction and Architecture, Slovak Academy of Sciences, 84503 Bratislava, Slovakia
[2] Center for Aerospace Research & Education, University of California, 5251 California Ave., Irvine, CA 92612, USA

tion is selected as the Heaviside step function or as the fundamental solution of the governing partial differential equations a pure contour integral formulation on local boundaries can be obtained for many boundary value problems in homogeneous solids. The local integral formulations with the use of a suitable fundamental solution have been successfully applied for isotropic elastostaticity [Zhu et al. (1998); Atluri et al. (2000), (2003)], elastodynamics [Sladek et al. (2003a,b)], heat conduction [Sladek et al. (2003c,d)], thermoelasticity [Sladek et al. (2001)] and plate bending problems [Sladek et al. (2002)] in homogeneous and nonhomogeneous solids.

The local boundary integral equation method to solve the heat conduction problem in an isotropic medium with a general variation of material properties has been presented in [Sladek et al. (2003c,d)]. Here, the previous method is extended to an anisotropic continuously nonhomogeneous medium. Since the fundamental solution for the considered governing equation is not available, a parametrix (Levi function) [Mikhailov (2002)] is applied to derive the integral representation for temperature. The parametrix correctly describes the main part of the fundamental solution but is not required to satisfy the original differential equation. In the present analysis we will use the steady fundamental solution for an anisotropic homogeneous solid [Sladek et al. (2003c)], which results in a boundary-domain integral formulation. Boundary-domain integral equations and the parametrix are applied to small subdomains, which cover the analyzed domain. On the boundary of subdomains (artificial boundary) lying in the interior of the body, both temperature and heat flux are unknown. To eliminate the number of unknowns on artificial boundaries the modified fundamental solution and/or the parametrix with a convenient cut-off function are applied. If the parametrix is vanishing on the boundary of the subdomain the integral containing the heat flux is removed from the integral representation. By choosing the Heaviside step function as the test function we obtain a pure contour integral formulation even for a nonhomogeneous solid problem under stationary conditions. In this approach the integral equations are applied only to internal nodes, and they have a very simple nonsingular form. The integration on a circular contour (boundary of the subdomains) is easily carried out. Boundary conditions for prescribed and unknown quantities on the global boundary are satisfied by collocating the approximate formulae at nodes on the global boundary. Hence, it is clear that there is no numerical integration necessary for the boundary nodes at all. These equations can be obtained in a natural way in the MLPG method, when the Dirac function is considered as the test function. By combining different test functions for internal and boundary nodes we obtain a computational method with a simple implementation.

Both methods are used to analyze steady and transient problems. In transient problems the Laplace transform technique is utilized to eliminate time variable in the differential equation. The spatial variation of the temperature is approximated by the moving least-square (MLS) scheme. Several quasi-static boundary value problems have to be solved for various values of the Laplace transform parameter. The Stehfest inversion method is applied to obtain the time-dependent solutions.

2 Local boundary integral equations

Consider a boundary value problem for the heat conduction problem in a continuously nonhomogeneous anisotropic medium, which in 2-d is described by the governing equation:

$$\rho(\mathbf{x})c(\mathbf{x})\frac{\partial\theta}{\partial t}(\mathbf{x},t) = [k_{ij}(x)\theta_{,j}(\mathbf{x},t)]_{,i} + Q(\mathbf{x},t), \qquad (1)$$

where $\theta(\mathbf{x},t)$ is the temperature field, $Q(\mathbf{x},t)$ is the density of body heat sources, k_{ij} is the thermal conductivity tensor, $\rho(\mathbf{x})$ is the mass density and $c(\mathbf{x})$ the specific heat. On the global boundary Γ, the following boundary and initial conditions are assumed

$$\theta(x,t) = \tilde{\theta}(x,t) \text{ on } \Gamma_\theta$$
$$q(x,t) = k_{ij}(x)\theta_{,j}(x,t)n_i(x) = \tilde{q}(x,t) \text{ on } \Gamma_q$$
$$\theta(x,t)|_{t=0} = \theta(x,0),$$

where n_i is the unit outward normal of the global boundary, Γ_θ is the part of the global boundary with prescribed temperature and on Γ_q the flux is prescribed.

Applying the Laplace transform to the governing equation (1), we have

$$\left[k_{ij}(\mathbf{x})\overline{\theta}_{,j}(\mathbf{x},p)\right]_{,i} - \rho(\mathbf{x})c(\mathbf{x})p\,\overline{\theta}(\mathbf{x},p) = -\overline{F}(\mathbf{x},p), \quad (2)$$

where

$$\overline{F}(\mathbf{x},p) = \overline{Q}(\mathbf{x},p) + \theta(\mathbf{x},0)$$

is the redefined body heat source in the Laplace transform domain with initial boundary condition for temperature and p is the Laplace transform parameter.

Instead of writing the global weak form for the above governing equation, the MLPG methods construct the weak form over local subdomains such as Ω_s, which is a small region taken for each node inside the global domain [Atluri and Shen (2002b)]. The local subdomains overlap each other, and cover the whole global domain Ω. The local subdomains could be of any geometric shape and size. In the current paper, the local subdomains are taken to be of circular shape. The local weak form of the governing equation (2) can be written as

$$\int_{\Omega_s} \left[\left(k_{ij}(\mathbf{x})\overline{\theta}_{,j}(\mathbf{x},p) \right)_{,i} - \rho(\mathbf{x})c(\mathbf{x})p\,\overline{\theta}(\mathbf{x},p) + \overline{F}(\mathbf{x},p) \right]$$
$$\cdot \theta^*(\mathbf{x})\,d\Omega = 0 , \qquad (3)$$

where $\theta^*(\mathbf{x})$ is a weight (test) function.

Applying the Gauss divergence theorem to eq. (3) one can write

$$\int_{\partial\Omega_s} \overline{q}(\mathbf{x},p)\theta^*(\mathbf{x})d\Gamma - \int_{\Omega_s} k_{ij}(\mathbf{x})\overline{\theta}_{,j}(\mathbf{x},p)\theta^*_{,i}(\mathbf{x})d\Omega$$
$$- \int_{\Omega_s} \rho(\mathbf{x})c(\mathbf{x})p\overline{\theta}(\mathbf{x},p)\theta^*(\mathbf{x})d\Omega$$
$$+ \int_{\Omega_s} \overline{F}(\mathbf{x},p)\theta^*(\mathbf{x})d\Omega = 0, \qquad (4)$$

where $\partial\Omega_s$ is the boundary of the local subdomain and

$$\overline{q}(\mathbf{x},p) = k_{ij}(\mathbf{x})\overline{\theta}_{,j}(\mathbf{x},p)n_i(\mathbf{x}) .$$

The local weak form (4) is a starting point to derive local boundary integral equations if an appropriate test function is selected.

2.1 The local symmetric weak form with Heaviside step function

If a Heaviside step function is chosen as the test function $\theta^*(\mathbf{x})$ in each subdomain

$$\theta^*(\mathbf{x}) = \begin{cases} 1 & \text{at } \mathbf{x} \in \Omega_s \\ 0 & \text{at } \mathbf{x} \notin \Omega_s \end{cases}$$

the local weak form (4) is transformed into a simple local boundary integral equation

$$\int_{\partial\Omega_s} \overline{q}(\mathbf{x},p)d\Gamma - \int_{\Omega_s} \rho(\mathbf{x})c(\mathbf{x})p\overline{\theta}(\mathbf{x},p)d\Omega$$
$$= - \int_{\Omega_s} \overline{F}(\mathbf{x},p)d\Omega. \qquad (5)$$

Equation (5) is recognized as the flow balance condition of the subdomain. In stationary case there is no domain integration involved in the left hand side of this local boundary integral equation. If the assumption of zero body heat sources is made, the pure contour integral formulation is obtained.

In the MLPG method the test and trial function are not necessarily from the same functional spaces. For internal nodes, the test function is chosen as the Heaviside step function with support on the local subdomain. The trial function, on the other hand, is chosen to be the moving least squares (MLS) interpolation over a number of nodes randomly spread within the domain of influence. While the local subdomain is defined as the support of the test function on which the integration is carried out, the domain of influence is defined as a region where the weight function is not zero and all nodes lying inside are considered for interpolation. The approximated function can be written as [Atluri and Shen (2002b)]

$$\overline{\theta}^h(\mathbf{x},p) = \mathbf{\Phi}^T(\mathbf{x}) \cdot \hat{\mathbf{\theta}}(p) = \sum_{a=1}^{n} \phi^a(\mathbf{x})\hat{\theta}^a(p) , \qquad (6)$$

where $\hat{\theta}^a(p)$ are fictitious parameters and $\phi^a(\mathbf{x})$ is the shape function associated with the node a. The number of nodes, n, used for the approximation of $\overline{\theta}(\mathbf{x},p)$ is determined by the weight function $w^a(\mathbf{x})$. A spline type weight function is considered in the present work

$$w^a(\mathbf{x})$$
$$= \begin{cases} 1 - 6\left(\frac{d^a}{r^a}\right)^2 + 8\left(\frac{d^a}{r^a}\right)^3 - 3\left(\frac{d^a}{r^a}\right)^4 & 0 \le d^a \le r^a \\ 0 & d^a \ge r^a \end{cases} ,$$

where $d^a = \|\mathbf{x} - \mathbf{x}^a\|$ and r^a is the size of the support domain.

The directional derivatives of $\overline{\theta}(\mathbf{x},p)$ are approximated in terms of the same nodal values as

$$\frac{\partial\overline{\theta}^h}{\partial n}(\mathbf{x},p) = n_k(\mathbf{x}) \sum_{a=1}^{n} \hat{\theta}^a(p)\phi^a_{,k}(\mathbf{x}). \qquad (7)$$

Making use of the MLS-approximation (6) and (7) for $\overline{\theta}(\mathbf{x}, p)$ and

$$q(\mathbf{x}, p) = k_{ij}(\mathbf{x})n_i(\mathbf{x}) \sum_{a=1}^{n} \hat{\theta}^a(p)\phi_{,j}^a(\mathbf{x}), \tag{8}$$

the local boundary integral equations (5) for all subdomains yields the following set of equations:

$$\sum_{a=1}^{n} \hat{\theta}^a(p) \int_{\partial\Omega_s} k_{ij}(\mathbf{x})n_j(\mathbf{x})\phi_{,j}^a(\mathbf{x})d\Gamma$$

$$- \sum_{a=1}^{n} \hat{\theta}^a(p) \int_{\Omega_s} \rho(\mathbf{x})c(\mathbf{x})p\phi^a(\mathbf{x})d\Omega$$

$$= - \int_{\Omega_s} \overline{F}(\mathbf{x}, p)d\Omega. \tag{9}$$

It should be noted that there are neither Lagrange multipliers nor penalty parameters introduced into the local weak form (3) because the essential boundary conditions on Γ_θ can be imposed directly using the interpolation approximation (6):

$$\sum_{a=1}^{n} \phi^a(\mathbf{x})\hat{\theta}^a(p) = \tilde{\overline{\theta}}(\mathbf{x}, p) \quad \text{for} \quad \mathbf{x} \in \Gamma_\theta. \tag{10}$$

Similarly one can obtain the equation for unknown $\hat{\theta}^a(p)$ at nodes from the global boundary where natural conditions are prescribed. Collocating the approximation (8) at $\mathbf{x} \in \Gamma_q$ one can write

$$k_{ij}(\mathbf{x})n_i(\mathbf{x}) \sum_{a=1}^{n} \hat{\theta}^a(p)\phi_{,j}^a(\mathbf{x}) = \tilde{\overline{q}}(\mathbf{x}, p). \tag{11}$$

Set of algebraic equations (9)-(11) is used for computation of the Laplace transform of fictitious parameters $\hat{\theta}^a(p)$.

2.2 *The local symmetric weak form with a fundamental solution*

Next, the test function is selected as the solution of the following equation

$$k_{ij}^s T_{,ij}(\mathbf{x}, \mathbf{y}) = -\delta(\mathbf{x}, \mathbf{y}) \tag{12}$$

which corresponds to steady heat conduction problems in a homogeneous body represented by k_{ij}^s and a body point heat source expressed by the Dirac delta function $\delta(\mathbf{x} - \mathbf{y})$. Its solution is given in an explicit form [Chang, Kang and Chen (1973)]:

$$T(\mathbf{x}, \mathbf{y}) = -\frac{\left|k^{ij}\right|^{1/2}}{2\pi} \ln R(\mathbf{x}, \mathbf{y}), \tag{13}$$

where

$$R^2 = k^{ij}(x_i - y_i)(x_j - y_j)$$

and k^{ij} is the inverse matrix to k_{ij}^s.

Adding and subtracting the term with a unifom heat conduction to the second term in equation (4), we obtain

$$\int_{\Omega_s} k_{ij}(\mathbf{x})\overline{\theta}_{,j}(\mathbf{x}, p)\theta_{,i}^*(\mathbf{x})d\Omega$$

$$= \int_{\Omega_s} \left(k_{ij} - k_{ij}^s\right) \overline{\theta}_{,j}(\mathbf{x}, p)\theta_{,i}^*(\mathbf{x})d\Omega$$

$$+ \int_{\Omega_s} k_{ij}^s \overline{\theta}_{,j}(x, p)\theta_{,i}^*(x)d\Omega.$$

Applying the Gauss divergence theorem to the last integral and taking into account the behaviour of the test function $\theta^* = T$ given by equation (12), one can write

$$\int_{\Omega_s} k_{ij}^s \overline{\theta}_{,j}(\mathbf{x}, p)\theta_{,i}^*(\mathbf{x})d\Omega$$

$$= \int_{\partial\Omega_s} k_{ij}^s T_{,i}(\mathbf{x}, \mathbf{y})n_j(\mathbf{x})\overline{\theta}(\mathbf{x}, p)d\Gamma$$

$$- \int_{\Omega_s} k_{ij}^s \overline{\theta}(\mathbf{x}, p)T_{,ij}(\mathbf{x}, \mathbf{y})d\Omega$$

$$= \int_{\partial\Omega_s} k_{ij}^s T_{,i}(\mathbf{x}, \mathbf{y})n_j(\mathbf{x})\overline{\theta}(\mathbf{x}, p)d\Gamma + \overline{\theta}(y, p).$$

Substituting these identities into equation (4), one can write the integral representation for Laplace transform of

temperature on a local subdomain

$$\overline{\theta}(\mathbf{y}, p) = \int\limits_{\partial\Omega_s} \overline{q}(\mathbf{x}, p) T(\mathbf{x}, \mathbf{y}) d\Gamma$$

$$- \int\limits_{\partial\Omega_s} \overline{\theta}(\mathbf{x}, p) k_{ij}^s n_j(\mathbf{x}) T_{,i}(\mathbf{x}, \mathbf{y}) d\Gamma$$

$$+ \int\limits_{\Omega_s} \overline{\theta}_{,j}(\mathbf{x}, p) \left[k_{ij}^s - k_{ij}(\mathbf{x}) \right] T_{,i}(\mathbf{x}, \mathbf{y}) d\Omega$$

$$- \int\limits_{\Omega_s} \rho(\mathbf{x}) c(\mathbf{x}) p \overline{\theta}(\mathbf{x}, p) T(\mathbf{x}, \mathbf{y}) d\Omega$$

$$+ \int\limits_{\Omega_s} \overline{F}(\mathbf{x}, p) T(\mathbf{x}, \mathbf{y}) d\Omega. \qquad (14)$$

The integral equations (14) are considered for small overlapping subdomains $\Omega_s \subset \Omega$. Hence, no of the boundary densities (Laplace transforms) are prescribed on the local boundary $\partial\Omega_s$ as long as it lies entirely inside Ω. The number of unknowns on $\partial\Omega_s$ in each LBIE can be reduced if a convenient weight function is introduced. If the fundamental solution in eq. (14) is vanishing on the boundary of subdomain the boundary integral containing the heat flux $\overline{q}(\mathbf{x}, p)$ is eliminated. One can see that the modified fundamental solution

$$T^*(\mathbf{x}, \mathbf{y}) = \frac{\left| k^{ij} \right|^{1/2}}{2\pi} \ln \frac{R_s}{R} \qquad (15)$$

is vanishing at (x_1^s, x_2^s) on the boundary of an ellipse centered at (y_1, y_2) and defined by

$$R_s^2 = k^{ij} (x_i^s - y_i)(x_j^s - y_j). \qquad (16)$$

The modified fundamental solution (15) is satisfying the governing equation (12). Then, the integral representation for temperature (14) will contain only temperatures under integrals if the fundamental solution $T(\mathbf{x}, \mathbf{y})$ is replaced by $T^*(\mathbf{x}, \mathbf{y})$. One can write:

$$\overline{\theta}(\mathbf{y}, p) = - \int\limits_{\partial\Omega_s} \overline{\theta}(\mathbf{x}, p) k_{ij}^s n_j(\mathbf{x}) T_{,i}^*(\mathbf{x}, \mathbf{y}) d\Gamma$$

$$+ \int\limits_{\Omega_s} \overline{\theta}_{,j}(\mathbf{x}, p) \left[k_{ij}^s - k_{ij}(\mathbf{x}) \right] T_{,i}^*(\mathbf{x}, \mathbf{y}) d\Omega$$

$$- \int\limits_{\Omega_s} \rho(\mathbf{x}) c(\mathbf{x}) p \overline{\theta}(\mathbf{x}, p) T^*(\mathbf{x}, \mathbf{y}) d\Omega$$

$$+ \int\limits_{\Omega_s} \overline{F}(\mathbf{x}, p) T^*(\mathbf{x}, \mathbf{y}) d\Omega. \qquad (17)$$

The geometry of the elliptical subdomain is given by eq. (16), where R_s is a free parameter. It should be selected in such a way that only one node is involved in the considered subdomain. The value of the conductivity tensor k_{ij}^s is taken as $k_{ij}(\mathbf{y})$. The main characteristics of the ellipse should be computed at each nodal point if nonhomogeneous material properties are considered. The integration over the boundary of ellipse, $\partial\Omega_s$, and over the domain Ω_s is more complex than integration over a simpler circular subdomain. It is the main reason why in the next part the circular domain is considered. Then, the modified fundamental solution $T^*(\mathbf{x}, \mathbf{y})$ is not vanishing on the circle with the radius R_s, what happens only for an isotropic case. For a general anisotropic medium one can use a parametrix [Mikhailov (2002)] instead of the modified fundamental solution. The parametrix correctly describes only the main part of the fundamental solution. Its form for a circular subdomain with radius r_0 can be given as

$$P(\mathbf{x}, \mathbf{y}) = \chi(r) T(\mathbf{x}, \mathbf{y}), \qquad (18)$$

where the cut-off function $\chi(r)$ can be selected as

$$\chi(r) = 1 - \frac{r^2}{r_0^2} \text{ with } r = |\mathbf{x} - \mathbf{y}| .$$

If the weight function θ^* in eq. (3) is replaced by the parametrix $P(\mathbf{x}, \mathbf{y})$, one obtains the integral representation for the Laplace transform of temperature

$$\overline{\theta}(\mathbf{y}, p) = - \int\limits_{\partial\Omega_s} \overline{\theta}(\mathbf{x}, p) k_{ij}^s n_j(\mathbf{x}) P_{,i}(\mathbf{x}, \mathbf{y}) d\Gamma$$

$$+ \int\limits_{\Omega_s} \overline{\theta}_{,j}(\mathbf{x}, p \left[k_{ij}^s - k_{ij}(\mathbf{x}) \right] P_{,i}(\mathbf{x}, \mathbf{y}) d\Omega$$

$$- \int\limits_{\Omega_s} \rho(\mathbf{x}) c(\mathbf{x}) p \overline{\theta}(\mathbf{x}, p) P(\mathbf{x}, \mathbf{y}) d\Omega$$

$$+ \int\limits_{\Omega_s} \overline{F}(\mathbf{x}, p) P(\mathbf{x}, \mathbf{y}) d\Omega$$

$$+ \int\limits_{\Omega_s} k_{ij}^s(\mathbf{x}) \left[(\chi - 1) T(\mathbf{x}, \mathbf{y}) \right]_{,ij} \overline{\theta}(\mathbf{x}, p) d\Omega. \qquad (19)$$

Performing the differentiation in the last integral in eq. (19) explicitly and making use of eq. (12) as well as

symmetry $k_{ij}^s = k_{ji}^s$, we may write

$$\int_{\Omega_s} k_{ij}(\mathbf{x})\left[(\chi-1)T(\mathbf{x},\mathbf{y})\right]_{,ij}\overline{\theta}(\mathbf{x},p)d\Omega$$

$$= -\frac{2}{r_0^2}k_{ij}^s\int_{\Omega_s}\overline{\theta}(\mathbf{x},p)\left[\delta_{ij}T(\mathbf{x},\mathbf{y})+2r_iT_{,j}(\mathbf{x},\mathbf{y})\right]d\Omega_s, \quad (20)$$

since the following identity is valid

$$\int_{\Omega_s} r^2 k_{ij}^s T_{,ij}(\mathbf{x},\mathbf{y})d\Omega = -\int_{\Omega_s} r^2\delta(r)d\Omega = 0$$

with respect to the governing equation for the fundamental solution (12).

Making use of the MLS-approximations (6) and (8) for $\overline{\theta}(\mathbf{x},p)$ and $\overline{q}(\mathbf{x},p)$, respectively, the local boundary integral equations (19) yield the following set of equations:

$$\sum_{a=1}^{n}\left\{\phi^a(\mathbf{y}^b)+\int_{\partial\Omega_s}k_{ij}^s n_j(\mathbf{x})P_{,i}(\mathbf{x},\mathbf{y}^b)\phi^a(\mathbf{x})d\Gamma\right\}\hat{\theta}^a(p)$$

$$=\sum_{a=1}^{n}\int_{\Omega_s}\left\{\left[k_{ij}^s - k_{ij}(\mathbf{x})\right]\phi_{,j}^a(\mathbf{x})P_{,i}(\mathbf{x},\mathbf{y}^b)\right.$$

$$-c(\mathbf{x})\rho(\mathbf{x})pP(\mathbf{x},\mathbf{y}^b)$$

$$\left.-\frac{2}{r_0^2}k_{ij}^s\left[\delta_{ij}T(\mathbf{x},\mathbf{y}^b)+2r_iT_{,j}(\mathbf{x},\mathbf{y}^b)\right]\right\}d\Omega\hat{\theta}^a(p)$$

$$+\int_{\Omega_s}\overline{F}(\mathbf{x},p)P(\mathbf{x},\mathbf{y}^b)d\Omega, \quad \text{for} \quad \mathbf{y}^b\in\Omega \quad (21)$$

At nodes on the global boundary, the following set of equations is used like in the previous formulation

$$\sum_{a=1}^{n}\phi^a(\mathbf{x})\hat{\theta}^a(p) = \tilde{\overline{\theta}}(\mathbf{x},p) \quad \text{for} \quad \mathbf{x}\in\Gamma_\theta.$$

$$k_{ij}(\mathbf{x})n_i(\mathbf{x})\sum_{a=1}^{n}\hat{\theta}^a(p)\phi_{,j}^a(\mathbf{x}) = \tilde{\overline{q}}(\mathbf{x},p) \quad \text{for} \quad \mathbf{x}\in\Gamma_q.$$

The time dependent values of the transformed variables can be obtained by an inverse transform. There are many inversion methods available for Laplace transform. As the Laplace transform inversion is an ill-posed problem, small truncation errors can be greatly magnified in the inversion process and lead to poor numerical results. In the present analysis the Stehfest algorithm [Stehfest (1970)] is used. An approximate value f_a of the inverse $f(t)$ for a specific time t is given by

$$f_a(t) = \frac{\ln 2}{t}\sum_{i=1}^{N}v_i\overline{f}\left(\frac{\ln 2}{t}i\right), \quad (22)$$

where

$$v_i = (-1)^{N/2+i}$$

$$\sum_{k=[(i+1)/2]}^{\min(i,N/2)}\frac{k^{N/2}(2k)!}{(N/2-k)!\,k!\,(k-1)!\,(i-k)!\,(2k-i)!}. \quad (23)$$

The selected number $N = 10$ with a single precision arithmetic is optimal to receive accurate results. It means that for each time t it is needed to solve N boundary value problems for the corresponding Laplace parameters $p = i\ln 2/t$, with $i = 1,2,...,N$. If M denotes the number of the time instants in which we are interested to know $f(t)$, the number of the Laplace transform solutions $\overline{f}(p_j)$ is then $M\times N$.
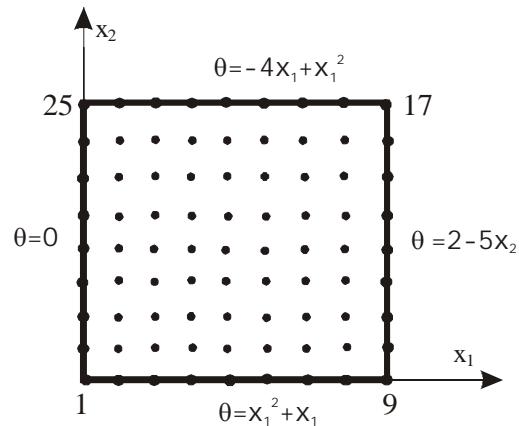

Figure 1 : Boundary conditions and node distribution for a square domain

3 Numerical examples

In this section numerical results will be presented to illustrate the implementation and effectiveness of both proposed methods. Firstly, homogeneous material properties and stationary boundary conditions are considered. An anisotropic square with homogeneous material properties is analyzed (Fig. 1). Dirichlet steady boundary conditions are prescribed on the whole boundary. In numerical solution we have considered a square with side $a = 0.01\,m$ and thermal conductivity tensor: $k_{11} = 1\times 10^{-4}, k_{22} = 1\times 10^{-4}$ and $k_{12} = 0.2\times 10^{-4}m^2s^{-1}$. For meshless approximation, 32 nodes were considered on the boundary and 49 nodes inside the investigated domain in both methods. A regular node distribution is used

(Fig. 1). The radius of circular subdomain is considered as $r_{loc} = 0.1 \times 10^{-2} m$.

This simple example was considered to obtain information about the accuracy of the present method. It can be easily shown that analytical solution

$$\theta = x_1^2 + x_1 - 5x_1x_2$$

satisfies the stationary counterpart of governing equation (1) for considered thermal conductivity tensor and prescribed boundary conditions shown in Fig. 1. The numerical results can be compared with analytical ones. The Sobolev norm of the temperature errors

$$r_\theta = \frac{\|\theta^{num} - \theta^{exact}\|}{\|\theta^{exact}\|} \times 100\% \qquad \text{with}$$

$$\|\theta\| = \left(\int_\Omega \theta \theta^d \Omega \right)^{1/2}$$

are 0,8% and 1,5% for formulations with test functions taken as Heaviside step function (labeled as MLPG5) and fundamental solution (MLPG6), respectively. The temperature distributions at three various x_2 coordinates 0,25; 0,5; 0,75 along the x_1 coordinate are shown in Fig. 2. One can observe excellent agreement of MLPG5 results with analytical ones. Figure 3 presents comparison both proposed methods, MLPG5 and MLPG6, with analytical solution. Both methods give very similar results.

A homogeneous anisotropic square domain (1×1) with vanishing heat flux on upper and bottom side, and prescribed temperature $\theta = 0$ and $\theta = 1$ on lateral left and right side, respectively , and thermal conductivity tensor: $k_{11} = 1, k_{22} = 1.5, k_{12} = 0.5$. Temperature variations with x_1 coordinate on upper and bottom sides are given in Fig. 4. In an isotropic square under the same boundary conditions a linear variation of temperature with x_1 coordinate can be observed. The Sobolev norm relative errors of MLPG5 and MLPG6 with respect to the FEM results is 0,87% and 1,83%, respectively. The FEM-NASTRAN results were obtained for a very fine mesh with 256 linear elements and we consider them to be accurate for homogeneous material properties.

The same geometry and boundary conditions are considered for a nonhomogeneous square domain, where $k_{11}(x_1) = 1 + x_1, k_{22} = 1.5, k_{12} = 0.5$. Temperature variations with x_1 coordinate on upper and bottom sides are
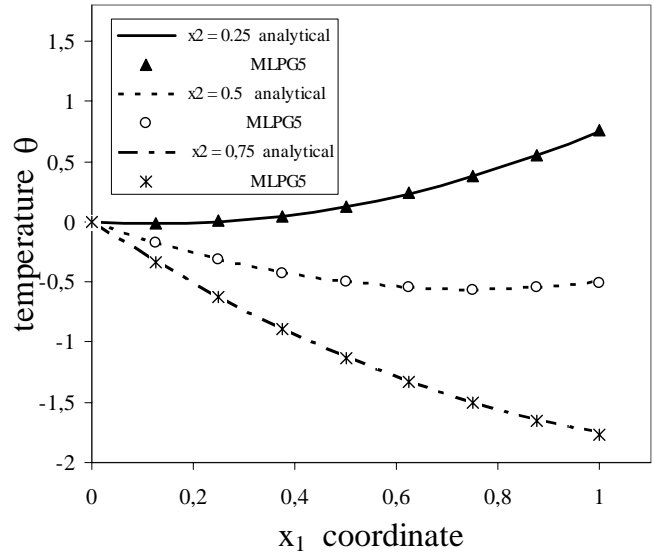

Figure 2 : Temperature distribution in a homogeneous anisotropic square
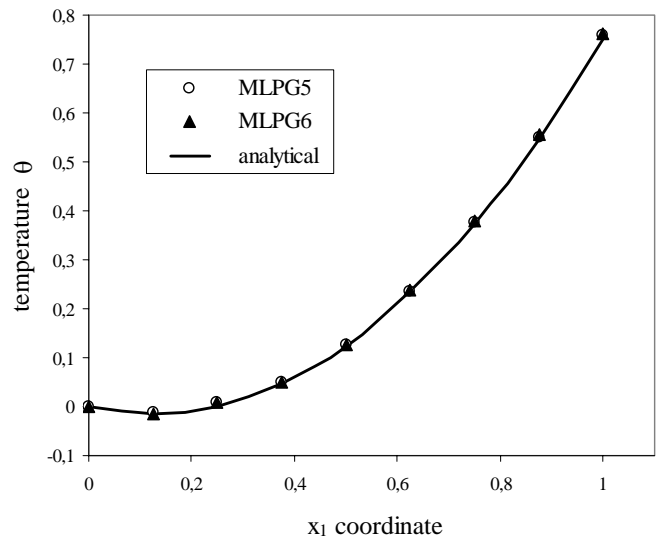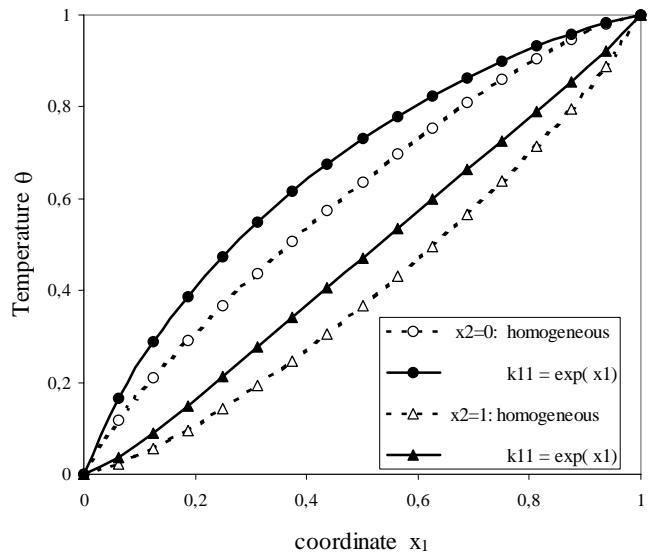

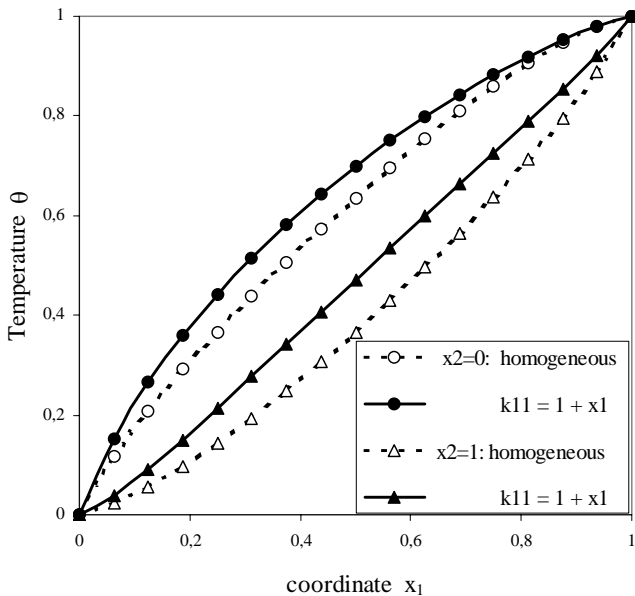**Figure 3** : Comparison of temperature distributions at $x_2 = 0.25$

given in Fig. 5. Numerical results were obtained by the MLPG5 method. The dashed lines correspond to a homogeneous case. If the thermal conductivity k_{11} is linearly growing with x_1 coordinate a higher temperature has to be received at smaller value of x_1 coordinate. It means that curves corresponding to nonhomogeneous case are shifted to left with respect to homogeneus case.
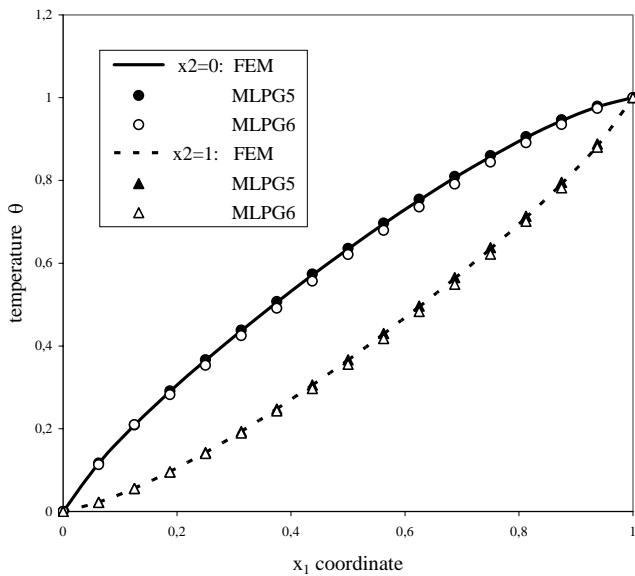
Figure 4 : Temperature variations with x_1 coordinate in a homogeneous anisotropic square domain

Figure 5 : Temperature variations with x_1 coordinate in a nonhomogeneous anisotropic square domain

Figure 6 : Temperature variations with x_1 coordinate in a nonhomogeneous anisotropic square domain with exponential variation of k_{11}

Transient heat conduction in an anisotropic square domain is analyzed too. Homogeneous material properties are considered: $k_{11} = 1$, $k_{22} = 1.5$, $k_{12} = 0.5$. The same boundary conditions as in the previous case are considered only a thermal shock represented by the Heaviside time step function is considered on the right lateral side of the square. The MLPG5 method is used to solve boundary value problems in the Laplace transform domain. The Stehfest inversion method is applied to obtain the time-dependent solutions at the mid of both upper and bottom sides of the square. Time variations of the temperature at $x_1 = 0.5$ in isotropic and anisotropic square domain are given in Fig. 7. For anisotropic material properties, temperature values are presented at bottom and upper sides of the square. It is clear that temperature is independent on x_2 for considered boundary conditions in an isotropic square.

4   Conclusions

A local boundary integral equation formulation in Laplace transform-domain with meshless approximation has been successfully implemented to solve 2-d initial-boundary value problems for transient heat conduction problem in anisotropic continuously non-homogeneous solids.

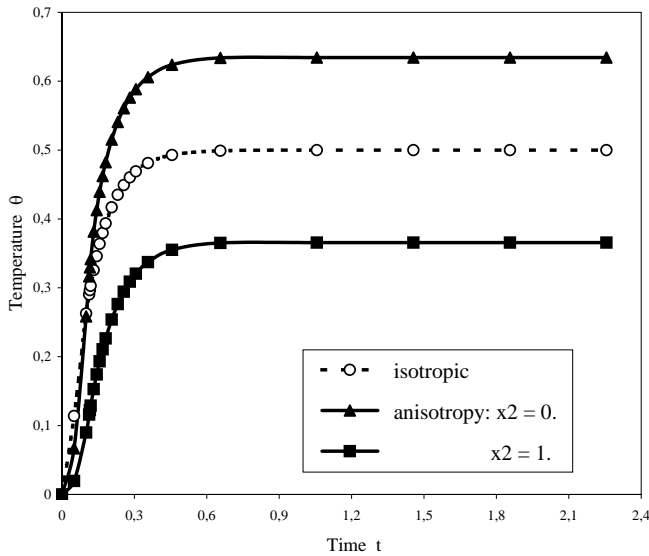An exponential variation of k_{11} thermal conductivity with x_1 coordinate is considered next: $k_{11} = \exp(\gamma x_1)$, $k_{22} = 1.5$, $k_{12} = 0.5$, where $\gamma = 1$. Numerical results are presented in Fig. 6. Character of curves is similar to previous case with linearly varying k_{11}.

Figure 7 : Time variations of the temperature in isotropic and anisotropic square domain

The Heaviside step function and parametrix are used, alternatively as test functions in the local symmetric weak form. It is leading to derive the local boundary-domain integral equations. No singularities are occurred in both formulations. The analyzed domain is divided into small overlapping circular sub-domains on which the local boundary integral equations are applied. The proposed methods are truly meshless methods, wherein no elements or background cells are involved in either the interpolation or the integration.

The method with the Heaviside step function as the test function is leading to a simpler integral formulation than in the case with the parametrix. The accuracy in the first method is a little higher than in the second one. The first method is leading to a pure contour integral method for stationary boundary conditions even for nonhomogeneous material properties, in contrast to the method with parametrix which contains boundary-domain integral equations.

The limitation of conventional boundary element approaches to homogeneous solids is removed by using the present local boundary integral equations. The computational accuracy of the present methods are comparable with that of FEM. However, the efficiency and the adaptability of the present methods are higher than in the conventional FEM because of eliminating the mesh genera-

tion troubles.

References

Atluri, S. N. (2004): *The Meshless Method(MLPG) for Domain & BIE Discretizations*, 688 pages, Tech Science Press, Forsyth, GA.

Atluri S. N., ; Shen S. (2002a): The Meshless Local Petrov-Galerkin (MLPG) Method: A Simple \& Less-costly Alternative to the Finite Element and Boundary Element Methods, *CMES: Computer Modeling in Engineering & Sciences*, 3: 11-52.

Atluri, S. N.; Shen, S. (2002b): *The Meshless Local Petrov-Galerkin (MLPG) Method*, Tech Science Press, Forsyth, GA.

Atluri, S. N.; Sladek, J.; Sladek, V.; Zhu, T. (2000): The local boundary integral equation (LBIE) and its meshless implementation for linear elasticity. *Comput. Mech.*, 25: 180-198.

Atluri, S. N.; Han, Z. D.; Shen, S. (2003): Meshless local Petrov-Galerkin (MLPG) approaches for solving the weakly-singular traction & displacement boundary integral equations. *CMES: Computer Modeling in Engineering & Sciences*, 4: 507-516.

Belytschko, T.; Lu, Y.; Gu, L. (1994): Element free Galerkin methods. *Int. J. Num. Meth. Engn.*, 37: 229-256.

Belytschko, T.; Krogauz, Y.; Organ, D.; Fleming, M.; Krysl, P. (1996): Meshless methods; an overview and recent developments. *Comp. Meth. Appl. Mech. Engn.*, 139: 3-47.

Brebbia, C. A.; Telles, J. C. F.; Wrobel, L. C. (1984): *Boundary Element Techniques*, Springer.

Chang, Y. P.; Kang, C. S.; Chen, D. J. (1973): The use of fundamental Green's functions for the solution of problems of heat conduction in anisotropic media. *J. Heat and Mass Transfer*, 16: 1905-1918.

Mikhailov, S. E. (2002): Localized boundary-domain integral formulations for problems with variable coefficients. *Engn. Analysis with Boundary Elements*, 26:

681-690.

Sladek, J.; Sladek, V.; Atluri, S. N. (2001): A pure contour formulation for the meshless local boundary integral equation method in thermoelasticity. *CMES: Computer Modeling in Engineering & Sciences*, 2: 423-434.

Sladek, J.; Sladek, V.; Mang, H. A. (2002): Meshless formulations for simply supported and clamped plate problems. *Int. J. Num. Meth. Engn.* 55: 359-375.

Sladek, J.; Sladek, V.; Van Keer, R. (2003a): Meshless local boundary integral equation method for 2D elastodynamic problems. *Int. J. Num. Meth. Engn.*, 57: 235-249.

Sladek, J.; Sladek, V.; Zhang, Ch. (2003b): Application of meshless local Petrov-Galerkin (MLPG) method to elastodynamic problems in continuously nonhomogeneous solids, *CMES: Computer Modeling in Engn. & Sciences*, 4: 637-648.

Sladek, J.; Sladek, V.; Zhang, Ch. (2003c): Transient heat conduction analysis in functionally graded materials by the meshless local boundary integral equation method. *Comput. Material Science*, 28: 494-504.

Sladek, J.; Sladek, V.; Krivacek, J.; Zhang, Ch. (2003d): Local BIEM for transient heat conduction analysis in 3-D axisymmetric functionally graded solids. *Comput. Mech.*, 32: 169-176.

Stehfest, H. (1970): Algorithm 368: numerical inversion of Laplace transform. *Comm. Assoc. Comput. Mach.*, 13: 47-49.

Sutradhar, A.; Paulino, G. H.; Gray, L. J. (2002): Transient heat conduction in homogeneous and non-homogeneous materials by the Laplace transform Galerkin boundary element method. *Engn. Analysis with Boundary Elements*, 26: 119-132.

Zhu, T.; Zhang, J. D.; Atluri, S. N. (1998): A Local Boundary Integral Equation (LBIE) Method in Computational Mechanics, and a Meshless Discretization Approach, *Computational Mechanics*, 21: pp. 223-235.